OUKA
The University of Osaka
Institutional Knowledge Archive

Title	Substrate recognition mechanisms of L-glutamate oxidase from Streptomyces sp. and its conversion to L-tyrosine oxidase
Author(s)	Ueda, Yuka; Yano, Yoshika; Nakayama, Natsume et al.
Citation	Protein Science. 2025, 35(1), p. e70432
Version Type	VoR
URL	https://hdl.handle.net/11094/103713
rights	This article is licensed under a Creative Commons Attribution-NonCommercial 4.0 International License.
Note	

The University of Osaka Institutional Knowledge Archive : OUKA

https://ir.library.osaka-u.ac.jp/

The University of Osaka

Check for updates

Received: 7 August 2025 | Revised: 3 December 2025 | Accepted: 6 December 2025

DOI: 10.1002/pro.70432

RESEARCH ARTICLE

THE PROTEIN SOCIETY WILEY

Substrate recognition mechanisms of L-glutamate oxidase from *Streptomyces* sp. and its conversion to L-tyrosine oxidase

Yuka Ueda[1] | **Yoshika Yano**[2] | **Natsume Nakayama**[2] | **Norihiro Takekawa**[1] | **Kenji Inagaki**[2] | **Katsumi Imada**[1]

[1]Department of Macromolecular Science, Graduate School of Science, The University of Osaka, Toyonaka, Osaka, Japan

[2]Department of Biofunctional Chemistry, Graduate School of Environmental and Life Science, Okayama University, Okayama, Okayama, Japan

Correspondence
Katsumi Imada, Department of Macromolecular Science, Graduate School of Science, The University of Osaka, 1-1 Machikaneyama-cho, Toyonaka, Osaka 560-0043, Japan.
Email: kimada@chem.sci.osaka-u.ac.jp

Funding information
Japan Society for the Promotion of Science, Grant/Award Number: 21K05278

Review Editor: Aitziber L. Cortajarena

Abstract

L-Amino acid oxidase (LAAO) is a flavoenzyme that catalyzes the oxidative deamination of L-amino acids, producing α-keto acids, ammonia, and hydrogen peroxide. Among LAAOs, L-glutamate oxidase (LGOX) from *Streptomyces* sp. X-119-6 exhibits exceptionally high substrate specificity for L-glutamate. LGOX is expressed as a homodimeric precursor and undergoes proteolytic processing for maturation. Structural studies revealed that LGOX comprises an FAD-binding domain, a substrate-binding domain, and a helical domain. Conserved residues W653, R124, and Y562 that recognize the α-amino and α-carboxyl groups of the substrate exist in the putative active site. R305 was identified as a key determinant for side-chain recognition; its substitution with Glu conferred specific activity toward L-arginine, effectively converting LGOX into an L-arginine oxidase. However, the putative substrate binding pocket includes an acidic residue, E617, undesirable for acidic substrates. Therefore, the mechanism of high specificity for L-glutamate remains unclear. To elucidate the molecular basis for the high substrate specificity of LGOX, we determined the structure of LGOX in complex with L-glutamate. Structural and mutational analyses revealed that E617 plays a critical role in substrate binding by aligning the side chain of R305. The loop at the entrance of the tunnel to the substrate-binding site regulates the access of the substrate to the site. Furthermore, E617F and E617K variants acquired L-tyrosine oxidase activity, providing insight into how specificity can be redirected. These findings clarify the substrate recognition mechanism of LGOX and underscore its potential as a robust scaffold for engineering novel amino acid oxidases with tailored specificities.

KEYWORDS
crystal structure, L-glutamate oxidase, modification of substrate specificity, substrate recognition

Yuka Ueda and Yoshika Yano contributed equally to this study.

This is an open access article under the terms of the Creative Commons Attribution-NonCommercial License, which permits use, distribution and reproduction in any medium, provided the original work is properly cited and is not used for commercial purposes.
© 2025 The Author(s). *Protein Science* published by Wiley Periodicals LLC on behalf of The Protein Society.

1 | INTRODUCTION

L-Amino acid oxidase (LAAO) is a flavoenzyme that catalyzes the oxidative deamination of L-amino acids to produce α-2-oxo acids with ammonia and hydrogen peroxide in the presence of molecular oxygen (Pollegioni et al., 2013). LAAOs have attracted considerable attention due to their broad biological activities and diverse biotechnological potential. Since it generates hydrogen peroxide, LAAOs exhibit antibacterial, antiviral (Kasai et al., 2015; Zhang et al., 2003), and antitumor effects (Amano et al., 2015; Lukasheva et al., 2021; Ullah, 2020), highlighting their potential as therapeutic agents (Kasai et al., 2021). In addition, LAAO is also expected to serve as a sustainable biocatalyst that could replace conventional chemical oxidation processes in the chemical industry (Al-Shameri et al., 2024).

LAAOs can be classified into two groups: those with low substrate specificity and those with high substrate specificity. Numerous low-specificity LAAOs have been reported from snake venoms (Izidoro et al., 2014), bacteria, and fungi (Yu & Qiao, 2012). In contrast, highly substrate-specific LAAOs are limited, including L-glutamate oxidase from *Streptomyces* sp. X-119-6 (LGOX; EC 1.4.3.11) (Kusakabe et al., 1983), L-lysine α-oxidase from *Trichoderma viride* Y244-2 (Kusakabe et al., 1980), L-aspartate oxidase from *Escherichia coli* (Nasu et al., 1982), L-tryptophan oxidase from *Chromobacterium violaceum* (Füller et al., 2016), L-phenylalanine oxidase from *Pseudomonas* sp. P-501 (Koyama, 1982), and L-arginine oxidase from *Pseudomonas* sp. TPU 7192 (Matsui et al., 2016). Among LAAOs, those with high substrate specificity have attracted particular attention. Highly substrate-specific LAAOs can serve as analytical tools and key components of biosensors for detecting specific L-amino acids in biological fluids, offering valuable biomarkers for autoimmune diseases, tumor progression, and immune response signaling (Matsui, 2023). Moreover, they can be used as the deracemization of amino acids for chiral compound synthesis (Al-Shameri et al., 2024). Therefore, novel LAAOs with high substrate specificity have been explored in nature (Pollegioni et al., 2013) and artificially created by mutations (Kondo et al., 2020; Yano et al., 2021). Recently, LAAO candidates have been discovered by in silico screening using genome databases, and novel LAAOs have been developed using an ancestral sequence reconstruction (ASR) method (Nakano, Minamino, et al., 2019; Nakano, Niwa, et al., 2019; Sugiura et al., 2021).

LGOX is a LAAO with the strictest substrate specificity and specifically catalyzes the oxidative deamination of L-glutamate in the presence of molecular oxygen, producing α-ketoglutarate via an amino acid intermediate, hydrogen peroxide, and ammonia. To date, LAAOs similar to LGOX have been reported in various actinomycete strains, such as *Streptomyces violascens* (Kamei et al., 1983), *Streptomyces endus* (Böhmer et al., 1989), *Streptomyces diastatochromogenes* (Wang et al., 2017), and *Streptomyces mobaraensis* (Liu et al., 2017). These enzymes are extracellular secreted proteins that are thermostable and pH-stable and contain noncovalently bound flavin adenine dinucleotide (FAD) as a cofactor. However, the molecular weights and subunit structures are rather different. LGOX is a homodimer with a molecular weight of approximately 70 kDa per subunit. LAAO from *S. violascens* is a monomer of about 62 kDa, and that from *S. endus* is a homodimer with subunits of approximately 45 kDa.

LGOX is expressed as a homodimeric precursor in the cell. This precursor is proteolytically processed by a metalloprotease into three fragments: α (A15–Y390, ∼40 kDa), β (G521–G683, ∼17 kDa), and γ (A391–A480, ∼10 kDa), which assemble into a mature heterohexameric enzyme with an $\alpha_2\beta_2\gamma_2$ structure. Both the precursor and mature forms exhibit strict specificity toward L-glutamate. However, the mature form shows dramatically enhanced activity toward L-glutamate and improved thermal stability (Arima et al., 2003; Arima et al., 2009). The structure of mature LGOX has already been determined at 3 Å resolution (Arima et al., 2009). LGOX consists of three domains: an FAD-binding domain (E17–G96, G332–T430, and Y621–A671), a substrate-binding domain (R97–R204, A324–G331, and H431–V620), and a helical domain (R205–R323). The putative active site contains residues W653, R124, and Y562, which are structurally conserved and correspond to the tryptophan, arginine, and tyrosine residues known to recognize the α-amino and α-carboxyl groups of the substrate in other LAAOs. Docking simulations between LGOX and L-glutamate based on the crystal structure suggested that R305 is involved in recognizing the side chain of L-glutamate (Arima et al., 2009). Mutant proteins in which R305 was substituted with A, L, D, E, or K exhibited little to no activity toward L-glutamate but showed activity toward L-histidine, L-phenylalanine, L-tyrosine, L-leucine, and L-arginine (Utsumi et al., 2012). Notably, the R305E variant demonstrated high oxidative activity toward L-arginine while showing negligible activity toward other amino acids, effectively acquiring properties characteristic of an L-arginine oxidase (Yano et al., 2021). Crystallographic analysis of the R305E protein and its complex with L-arginine revealed that the α-amino and α-carboxy groups of the substrate are recognized by the conserved residues W653, R124, and Y562, while the side chain of L-arginine is recognized by the mutated E305, along with D433 and E617 (Yano et al., 2021). These findings indicate that R305 is a key residue responsible for the strict substrate specificity of LGOX. However, the full molecular basis for the high substrate specificity of LGOX remains unclear. In particular, an acidic residue, E617, is exposed on the surface of the putative substrate binding pocket. This is

1469896x, 2026, 1, Downloaded from https://onlinelibrary.wiley.com/doi/10.1002/pro.70432 by The University Of Osaka, Wiley Online Library on [07/01/2026]. See the Terms and Conditions (https://onlinelibrary.wiley.com/terms-and-conditions) on Wiley Online Library for rules of use; OA articles are governed by the applicable Creative Commons License

undesirable for L-glutamate recognition. Therefore, the mechanism of highly specific recognition for L-glutamate by LGOX is still obscure.

To address this, we determined the crystal structure of LGOX in complex with L-glutamate. The structure and the mutational analyses revealed the molecular basis of the high specificity of LGOX for L-glutamate and indicated that E617 is a critical residue in substrate recognition. Furthermore, the mutational analysis showed that the E617F and E617K variants of LGOX acquired L-tyrosine oxidase activity. Structural analysis of these variants allowed us to infer the determinants of substrate specificity. Taken together with previous findings on the R305E mutant, these results demonstrate that LGOX serves as a promising template for the rational design of novel amino acid oxidases with high substrate specificity.

2 | RESULTS

2.1 | Crystallization of LGOX in complex with L-glutamate

The ligand-free structure of LGOX was elucidated approximately 15 years ago (Arima et al., 2009); however, reproducible crystals suitable for X-ray crystallographic analysis had not been obtained since then. To overcome this, we modified the expression plasmid, altered the purification procedure, and replaced the protease used for maturation. In previous preparations, two types of α-fragments were generated after maturation, but in the current preparation used for crystallization, the α-fragment appeared predominantly as a single band corresponding to the lower molecular weight form on SDS-PAGE (Figure S1). We used metalloprotease from *Streptomyces griseus* (Kaken Pharmaceutical Co., Ltd., Tokyo, Japan) at 4% (w/w) relative to the protein and stored it at 30°C for maturation. The control of the digestion condition was essential to obtain the single-band α-fragment. This may explain why we were able to obtain crystals suitable for X-ray crystallographic analysis this time.

2.2 | Structure of LGOX in complex with L-glutamate

The crystals of the L-glutamate complex of LGOX were prepared by the soaking method. The yellow color of the LGOX crystals disappeared after 5–10 min soaking in a solution containing 10 mM of L-glutamate, indicating that FAD is converted to the reduced form and that the substrate is bound to the enzyme (Kondo et al., 2020; Moustafa et al., 2006; Yano et al., 2021). We collected the X-ray diffraction data from the colorless crystals. Although the crystallization condition of the LGOX crystals used for soaking differs from the previous crystallization condition, the L-glutamate complex crystal belongs to the same space group of $P6_122$ with almost the same cell dimensions of $a = b = 124.3$ and $c = 168.8$ Å (Table S1) as in the previous study (Arima et al., 2009).

The crystal structure of LGOX with L-glutamate was determined at 2.55 Å resolution (Figures 1a and S1). The final model includes residues M18–G363 and G375–E386 in α-fragment (A15–Y390), all residues in γ-fragment (A391–A480), and residues G521–V673 in β-fragment (G521–G683). The residues A15–E17, R364–P374, G387–Y390, and G674–G683 were not modeled due to poor electron density. A single mature LGOX protomer exists in an asymmetric unit, and two LGOX protomers related by crystallographic two-fold symmetry form a dimer (Figure S1c), as the structure of substrate-free LGOX (Arima et al., 2009).

The Cα backbone trace of the glutamate complex is almost identical to that of substrate-free LGOX, except for the loop region (F314–T325) connecting the helical domain with the substrate binding domain (Figure 1b–d). This loop forms one side of the entrance of the tunnel leading to the substrate-binding site and, therefore, is hereafter referred to as the "entrance loop." In the substrate-free LGOX structure, the entrance to the substrate-binding site is widely open; however, in the substrate complex, the position of the entrance loop is shifted, resulting in a narrower tunnel entrance.

L-glutamate is located on the isoalloxazine ring of FAD (Figure 2a,b), as expected from the structure of the R305E variant with L-arginine (Yano et al., 2021). The α-carboxy group of the L-glutamate hydrogen-bonds with R124 and Y562, and the α-amino group of L-glutamate binds to the α-carbonyl oxygen of A652 and the indole ring of W653 through a cation-π interaction. These interactions are conserved in other LAAOs (Geueke & Hummel, 2002; Moustafa et al., 2006). The γ-carboxy group of L-glutamate forms hydrogen bonds with R305, H312, and E617. E617 also forms a hydrogen bond with the guanidino group of R305, reducing the negative charge of E617 and enabling the direct interaction with the L-glutamate side chain. The side chain of R305 adopts an extended conformation to interact with the L-glutamate side chain. The extended conformation is stabilized by hydrogen bonds with E617 and D433 and a cation-π stacking interaction between the guanidino group of R305 and the indole ring of W564. This hydrophilic interaction network contributes to the high affinity of LGOX for L-glutamate.

2.3 | Effect of mutation at H312 and D433 on the enzyme property of LGOX

H312 and D433 are involved in the hydrogen bonding network that recognizes the side chain of L-glutamate (Figure 2a,b). To evaluate the contribution of these

1469896x, 2026, 1, Downloaded from https://onlinelibrary.wiley.com/doi/10.1002/pro.70432 by The University Of Osaka, Wiley Online Library on [07/01/2026]. See the Terms and Conditions (https://onlinelibrary.wiley.com/terms-and-conditions) on Wiley Online Library for rules of use; OA articles are governed by the applicable Creative Commons License

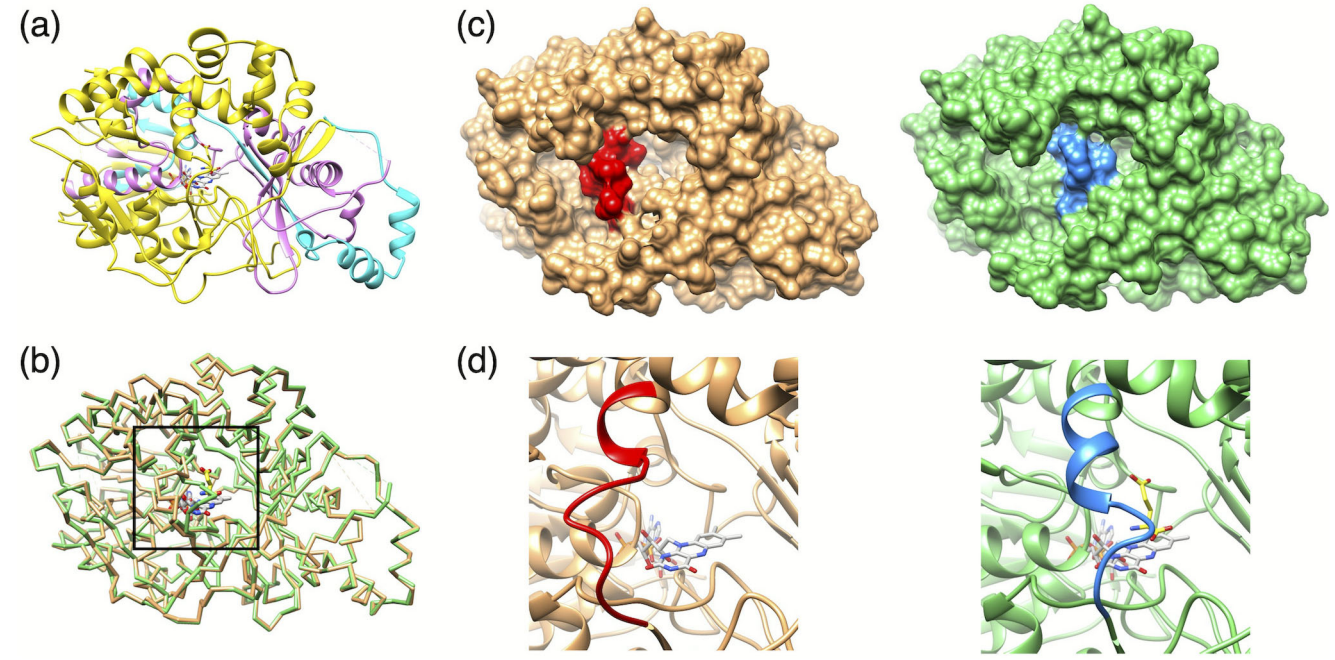

FIGURE 1 Structural comparison of LGOX and the L-glutamate complex of LGOX. (a) Ribbon representation of the L-glutamate complex of LGOX. α-, β-, and γ-fragments are colored in yellow, magenta, and cyan, respectively. (b) Superposition of Cα traces of LGOX (orange) and the L-glutamate complex of LGOX (green). (c) Surface representation of LGOX (the left panel) and the L-glutamate complex of LGOX (the right panel) viewed from the entrance of the substrate. The entrance loop (F314–T325) is colored in red (LGOX) and blue (LGOX with L-glutamate). (d) Close-up views of the entrance of the substrate indicated by the black box in (b): the left panel, LGOX; the right panel, L-glutamate complex of LGOX. The colors are the same as (c). FAD and L-glutamate are shown by stick model colored by element: red, oxygen; blue, nitrogen; gray, carbon of FAD; yellow, carbon of L-glutamate. LGOX, L-glutamate oxidase.

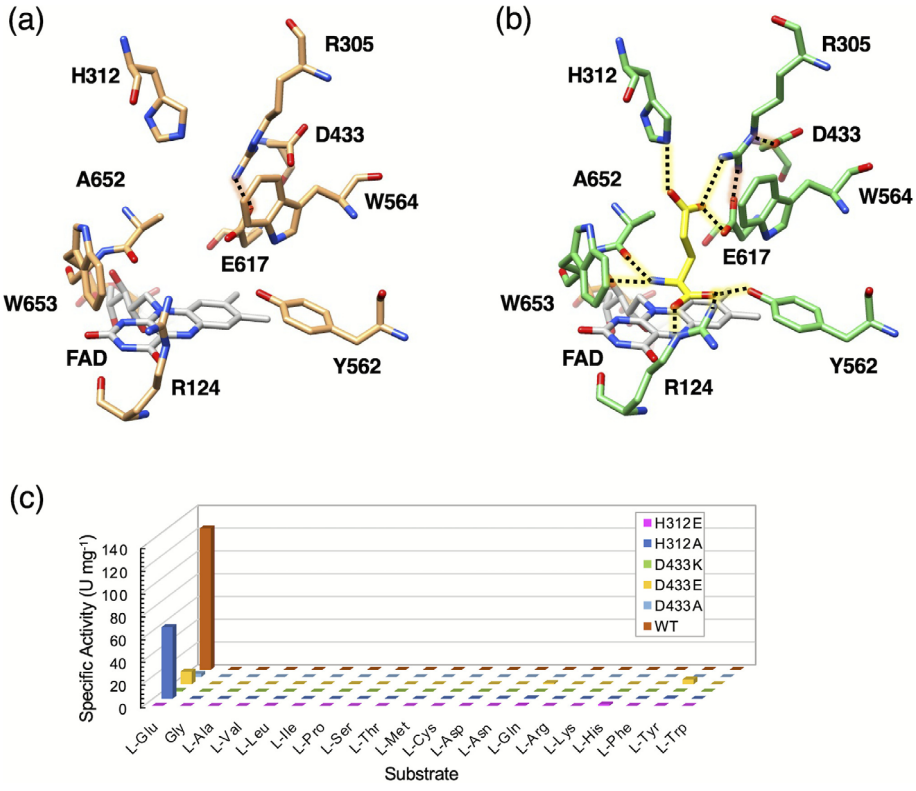

FIGURE 2 L-glutamate recognition by LGOX. (a, b) Structures of the substrate-binding site are shown by stick model in orange for substrate-free LGOX (a) and green for LGOX complexed with L-glutamate (b). FAD and L-glutamate are colored in light gray and yellow, respectively. The nitrogen and oxygen atoms are colored in blue and red, respectively. Possible hydrogen bonds are indicated by dotted lines. (c) Effect of mutation at H312 or D433 on substrate specificity of LGOX. Specific activities of H312E, H312A, H312K, H312E, H312A, and wild-type LGOX are indicated in magenta, blue, green, orange, light blue, and brown bars, respectively. Enzyme activities were measured by the 4-aminoantipyrine phenol method using 5 mM substrates in KPB (pH 7.4) at 40°C. KPB, potassium phosphate buffer; LGOX, L-glutamate oxidase.

1469896x, 2026, 1, Downloaded from https://onlinelibrary.wiley.com/doi/10.1002/pro.70432 by The University Of Osaka, Wiley Online Library on [07/01/2026]. See the Terms and Conditions (https://onlinelibrary.wiley.com/terms-and-conditions) on Wiley Online Library for rules of use; OA articles are governed by the applicable Creative Commons License

TABLE 1 Kinetic parameters of the LGOX mutants.

Variants	Substrate	Specific activity (U mg^{-1})	K_m (mM)	k_{cat} (s^{-1})	k_{cat}/K_m (M^{-1} s^{-1})
WT	L-glutamate	124	0.19 ± 0.04	151 ± 49	7.9×10^5
D433E	L-glutamate	11	5.4	95	1.8×10^4
D433A	L-glutamate	2.9	2.0	31	1.5×10^4
D433K	L-glutamate	0.8	8.9	2	1.8×10^2
E617Q	L-glutamate	88	0.10 ± 0.01	80 ± 2	8.0×10^5
E617N	L-glutamate	51	0.83	38	4.6×10^4
E617L	L-glutamate	43	0.19	31	1.7×10^5
E617V	L-glutamate	31	0.63	39	6.2×10^4
E617M	L-glutamate	29	0.43	160	3.7×10^5
E617K	L-tyrosine	12	1.1 ± 0.4	3.2 ± 1.3	2.9×10^3
E617F	L-tyrosine	16	0.84 ± 0.08	18.5 ± 0.7	2.2×10^4

Note: Kinetic parameters were calculated by fitting the data to the Michaelis–Menten equation using Solver in Microsoft Excel (Microsoft Co.). The initial velocities at each substrate concentration were measured three times for the determination of the kinetic parameters. The kinetic parameters of WT (wild type), E617Q, E617K, and E617F were determined using two independently purified protein samples, and the others were determined using a single protein sample.

residues to the substrate binding, we prepared H312A, H312E, D433A, D433E, and D433K mutant proteins and analyzed their activity toward L-glutamate (Figure 2c, Table 1). The H312A mutation reduced the activity toward L-glutamate to 40% of the wild type, and the H312E mutation completely abolished it. The activities of D433E, D433A, and D433K mutant proteins were reduced by less than 7% compared with the wild type. These results indicate that H312 and D433 contribute to the recognition of L-glutamate. The K_m value of D433A (2.0 mM) increased 11 times that of the wild type (0.19 mM), whereas the k_{cat} value (31 s^{-1}) reduced 20% of that of the wild type (151 s^{-1}) (Table 1, Figure S2). Therefore, D433 contributes to the binding affinity for L-glutamate, although D433 has no direct interaction with L-glutamate (Figure 2b).

2.4 | Enzyme properties of E617X mutant variants of LGOX

The crystal structure showed that E617 directly interacts with the substrate as well as aligns the guanidino group of R305, suggesting the contribution of E617 to substrate recognition (Figure 2b). To elucidate the importance of E617 on the strict substrate specificity of LGOX, we conducted saturated mutagenesis at E617 of LGOX (E617X) and evaluated the enzyme properties of the mutant proteins. We determined the specific activity of E617X proteins against the 20 amino acids by the 4-aminoantipyrine phenol method (Figure 3). The E617X mutation, except for E617Q, significantly decreased the specific activity of LGOX against L-glutamate, indicating the importance of E617 for the L-glutamate recognition. Most of the E617X mutant variants show activity to L-glutamate of less than 20% of the wild type while maintaining strict specificity for L-glutamate. However, the E617K, E617F, E617M, E617L, and E617V proteins acquired significant activity against L-tyrosine. The E617K and E617F proteins have the highest activity for L-tyrosine, seven times higher than L-glutamate, whereas the E617M protein shows a similar level of activity for L-glutamate and L-tyrosine (Figure 3). The apparent K_m value of the E617Q protein for L-glutamate (0.10 mM) is about half of that of the wild type (0.19 mM), and the k_{cat} value (80 s^{-1}) is also about half of that of the wild type (151 s^{-1}) (Table 1, Figure S2). Therefore, the specificity constant of the E617Q protein is almost the same level as that of the wild type. This result is probably due to the loss of the negative charge upon substitution of Q for E.

2.5 | Structures of LGOX E617Q with and without substrate

To elucidate the structural basis for the enhanced specificity constant of the E617Q mutant variant, we determined the crystal structures of the E617Q variant with and without L-glutamate at 2.43 and 2.38 Å resolution (Figure 4), respectively, and compared them with those of the wild type. The structure of the E617Q variant is very similar to that of the wild type. The conformation of the entrance loop resembles that of the wild type, and therefore, the entrance to the active site is open (Figure 4a). However, the region composed of residues Y562 to R579 shifted by approximately 1 Å (Figure 4b). As a result, Y562 moved slightly, while W564 underwent a more significant displacement, leading to an expansion of the substrate-binding site compared with the wild type (Figures 2a and 4c).

The structure of the L-glutamate complex of the E617Q variant is nearly identical to that of the wild type,

1469896x, 2026, 1, Downloaded from https://onlinelibrary.wiley.com/doi/10.1002/pro.70432 by The University Of Osaka, Wiley Online Library on [07/01/2026]. See the Terms and Conditions (https://onlinelibrary.wiley.com/terms-and-conditions) on Wiley Online Library for rules of use; OA articles are governed by the applicable Creative Commons License

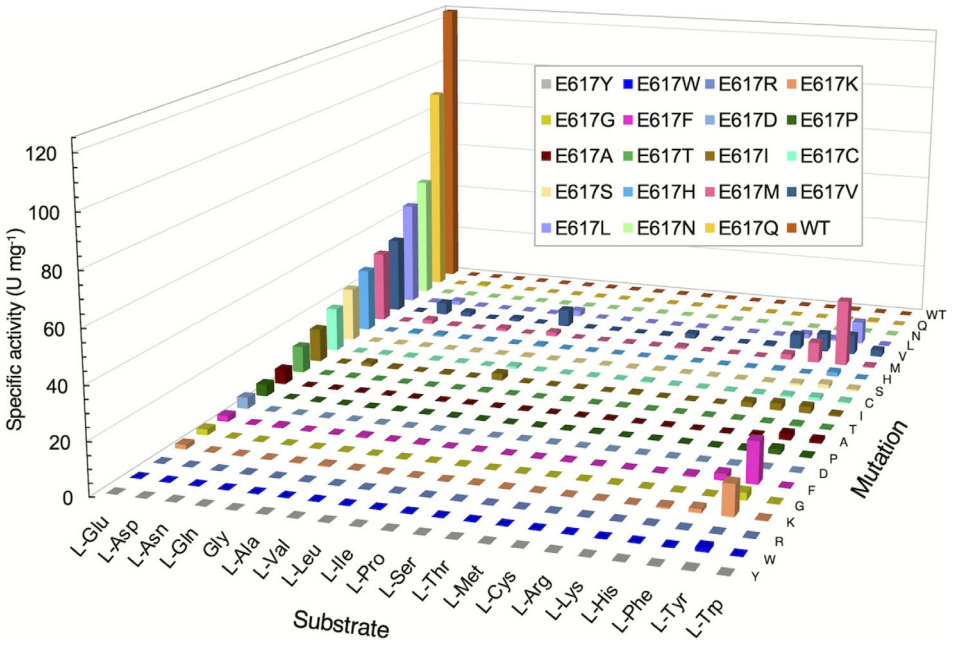

FIGURE 3 Effect of mutation at E617 on substrate specificity of LGOX. Specific activities of E617X variants against the 20 amino acids are shown by a 3D bar graph. Enzyme activities were measured by the 4-aminoantipyrine phenol method using 5 mM substrates in KPB (pH 7.4 or pH 8.0) at 40°C. KPB, potassium phosphate buffer; LGOX, L-glutamate oxidase.

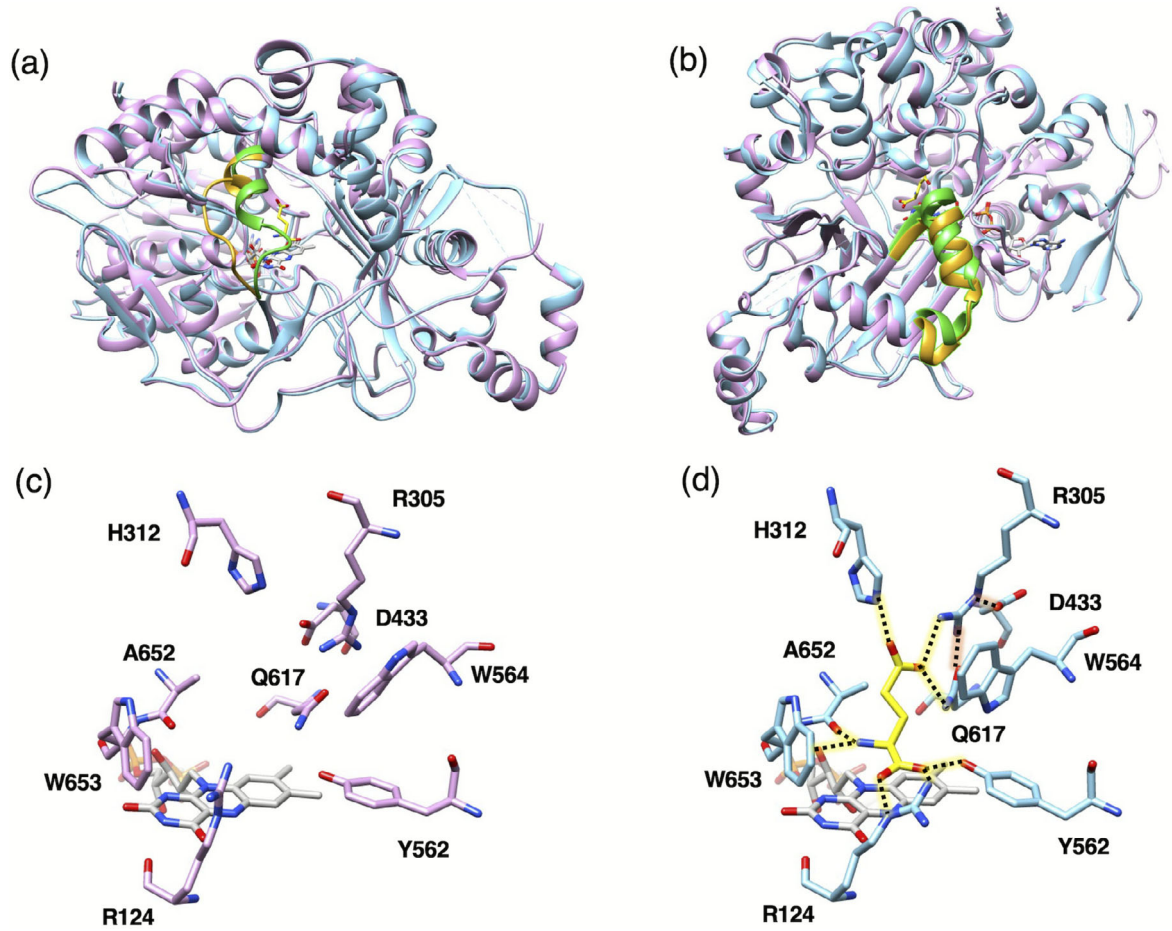

FIGURE 4 Structural comparison of the E617Q variant and its L-glutamate complex. (a) Ribbon models of the E617Q variant (magenta) and its L-glutamate complex (cyan) are superimposed. The entrance loop region (F314–T325) of the E617Q variant and that of the L-glutamate complex are colored in orange and green, respectively. (b) View from the backside of (a). The segment from Y562 to R579 of the E617Q variant and that of the L-glutamate complex are colored in orange and green, respectively. (c, d) Structures of the substrate-binding site are shown by stick model in magenta for the substrate-free E617Q variant (c) and cyan for the L-glutamate complex (d). FAD and L-glutamate are colored in light gray and yellow, respectively. The nitrogen and oxygen atoms are colored in blue and red, respectively. Possible hydrogen bonds are indicated by dotted lines.

14698896c, 2026, 1, Downloaded from https://onlinelibrary.wiley.com/doi/10.1002/pro.70432 by The University Of Osaka, Wiley Online Library on [07/01/2026]. See the Terms and Conditions (https://onlinelibrary.wiley.com/terms-and-conditions) on Wiley Online Library for rules of use; OA articles are governed by the applicable Creative Commons License

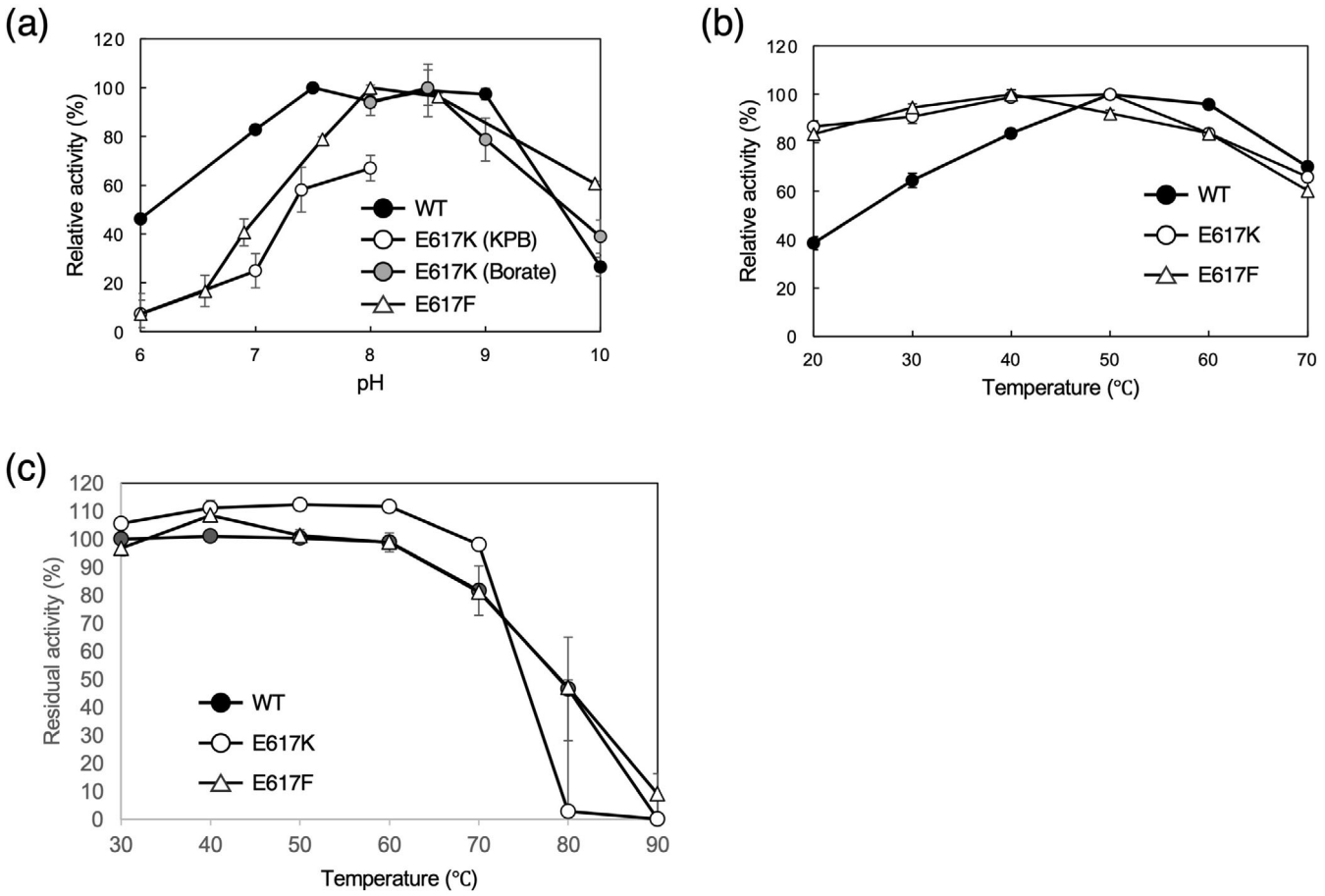

FIGURE 5 Enzyme properties of the E617F and E617K variants. (a) Effect of pH on the enzyme activities of WT, E617F, and E617K. The activity at the optimum pH was set as 100% relative activity. (b) Temperature dependence of the enzyme activities of WT, E617F, and E617K. Relative activities at pH 7.4 from 20°C to 70°C are plotted. The maximal activity is set as 100% relative activity (40°C for E617F and E617K and 50°C for WT). (c) The residual activities after incubation at various temperatures (30°C–90°C) for 1 h. Relative activities of WT, E617F, and E617K are plotted. The activity without heat treatment was set as 100% residual activity. The enzyme activities at each condition were measured three times in all the experiments, and the averaged values were plotted. The biological replicate was one.

with the entrance loop narrowing the entrance to the substrate-binding site in the same manner as in the wild type. The L-glutamate is bound to the E617Q protein in a similar manner to the wild type (Figures 2b and 4d). The γ-carboxy group of L-glutamate forms hydrogen bonds with R305, H312, and Q617. Q617 also forms a hydrogen bond with R305, which in turn interacts with D433 and W564. Therefore, the relatively low K_m value of the E617Q protein is attributed to the loss of negative charge caused by the substitution of glutamic acid (E) with glutamine (Q).

2.6 | Structures and enzyme properties of E617F and E617K variants

The E617F and E617K mutant proteins not only showed reduced activity toward L-glutamate but also acquired activity for L-tyrosine. Therefore, we investigated the enzymatic properties of the E617F and E617K variants with respect to L-tyrosine (Figure 5, Table 1). The specific activities toward L-tyrosine determined by the 4-aminoantipyrine phenol method were 12 U mg^{-1} for E617K and 16 U mg^{-1} for E617F. The optimal pH was 8.5 for E617K and 8.0 for E617F, but both mutant proteins showed a sharp decline in activity at pH 7 (Figure 5a). The optimal reaction temperatures were 50°C for E617K and 40°C for E617F, slightly lower than that of the wild type for L-glutamate (Figure 5b). Both mutant proteins maintained relatively high activity across the 20°C–40°C range. Furthermore, the E617K and E617F variants retained approximately 80% of their activity after heat treatment at 70°C for 1 h, demonstrating thermal stability comparable to that of the wild type (Figure 5c). The K_m values for L-tyrosine were 0.84 mM for E617F and 1.1 mM for E617K, whereas the k_{cat} values were similar (18.5 s^{-1} for E617F and 3.2 s^{-1} for E617K), resulting in a higher catalytic efficiency for E617F (Table 1, Figure S2). These values are comparable to those reported for

14698896c, 2026, 1, Downloaded from https://onlinelibrary.wiley.com/doi/10.1002/pro.70432 by The University Of Osaka, Wiley Online Library on [07/01/2026]. See the Terms and Conditions (https://onlinelibrary.wiley.com/terms-and-conditions) on Wiley Online Library for rules of use; OA articles are governed by the applicable Creative Commons License

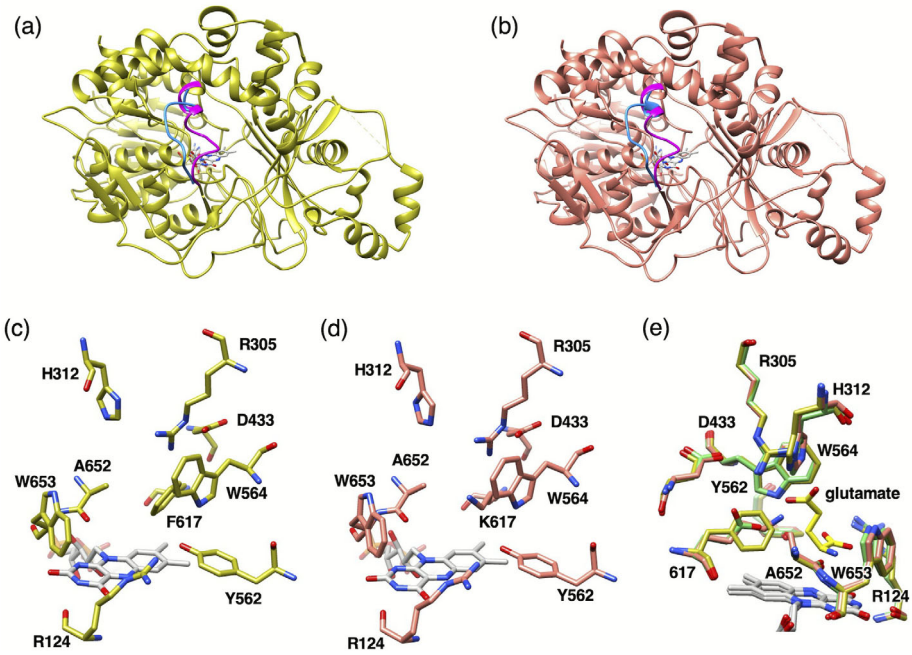

FIGURE 6 Structural comparison of E617F and E617K variants. (a, b) Ribbon representation of the E617F variant (a) and the E617K variant (b). The two alternative structures of the entrance loop region (F314–T325) are highlighted in cyan and magenta. (c, d) Structures of the substrate-binding site are shown by stick model in yellow for the E617F variant (c) and brown for the E617K variant (d). (e) Superimposition of the substrate-binding site of the L-glutamate complex of wild-type LGOX (green), the E617F variant (yellow), and the E617K variant (brown) viewed from the left side of (c). FAD and L-glutamate are colored in light gray and yellow, respectively. The nitrogen and oxygen atoms are colored in blue and red, respectively. LGOX, L-glutamate oxidase.

low-substrate-specificity LAAOs (Chen et al., 2012; Duerre & Chakrabarty, 1975; El-Sayed et al., 2013; Geueke & Hummel, 2002; Mandal & Bhattacharyya, 2008; Mizon et al., 1970; Wei et al., 2007; Wei et al., 2009) and LysOX D212A/D315A (Nakano, Niwa, et al., 2019). Notably, the E617F and E617K variants exhibit strict substrate specificity for L-tyrosine, suggesting that these mutations effectively converted the enzyme into a L-tyrosine oxidase.

Next, we determined the crystal structures of the E617F and E617K variants at 3.27 and 1.85 Å resolutions, respectively (Figure 6a,b). Unfortunately, the X-ray data of L-tyrosine complex crystals were not obtained due to serious damage from soaking. The overall structures of the E617F and E617K variants resemble the substrate-free structure of the wild type. Both mutant proteins show alternative conformations in the entrance loop: one is an open conformation, and the other is a closed conformation, suggesting the flexibility of the entrance loop. The active site structures of the E617F and E617K variants are nearly identical to that of the wild type (Figures 2a and 6c,d). The side chains of K617 and F617 locate positions that overlap with that of E617 in the wild type. Due to their slightly bulkier side chains, the tips of K617 and F617 extend slightly toward the center of the binding site (Figure 6e). The reduced activity toward L-glutamate is likely due to steric hindrance caused by this protrusion, which prevents L-glutamate from binding in the same position and conformation as in the wild type. Meanwhile, the active site appears to have sufficient space to accommodate the side chain of L-tyrosine. The side chain of H312 and the main chain carbonyl oxygen of H651 are positioned at the upper part of the active site, potentially allowing interactions with the hydroxyl group of the L-tyrosine side chain. Additionally, in the E617K protein, K617 may stabilize the tyrosine side chain via cation–π interaction, while in the E617F protein, stabilization may occur through π–π stacking with F617. However, to fully elucidate the mechanism of specificity toward L-tyrosine, structural analysis of the substrate-bound complex is necessary.

3 | DISCUSSION

The structure of the L-glutamate complex of LGOX, along with the structural and enzymatic studies of the variant proteins with mutation at residues interacting with the L-glutamate side chain, revealed the structural basis for the strict substrate specificity of LGOX toward L-glutamate. The recognition of the α-amino and α-carboxyl groups of L-glutamate is identical to that in other L-amino acid oxidases (LAAOs) and is structurally well conserved (Figure 2). The γ-carboxy group of L-glutamate forms hydrogen bonds with H312, R305, and E617. The position of R305 is precisely defined through interactions with D433, E617, and W564. These interactions immobilize L-glutamate in a position optimal for the reaction, thereby contributing to the high activity toward L-glutamate (Figure 2). Experimental results from the H312, D433, and E617 mutant proteins support this mechanism. Mutations at H312, D433, and E617 significantly reduced activity toward L-glutamate (Figure 2c). In particular, the marked decrease in activity observed with the D433 mutant protein, despite D433 not directly interacting with L-glutamate, suggests that the alignment of R305 is critical for catalysis. Although E617 carries a negative charge, which would

1469896x, 2026, 1, Downloaded from https://onlinelibrary.wiley.com/doi/10.1002/pro.70432 by The University Of Osaka, Wiley Online Library on [07/01/2026]. See the Terms and Conditions (https://onlinelibrary.wiley.com/terms-and-conditions) on Wiley Online Library for rules of use; OA articles are governed by the applicable Creative Commons License

seem unfavorable for binding L-glutamate, it contributes to the alignment of R305. Once the negative charge is partially shielded by R305, E617 can directly interact with the glutamate side chain and play a crucial role in substrate specificity. The results from the E617 mutant proteins further support this role: the E617Q variant, which lacks the negative charge but has a side chain size similar to glutamate, exhibited even higher catalytic efficiency toward L-glutamate than the wild type (Table 1). Structural analysis of the E617Q variant confirmed that all interactions with L-glutamate observed in the wild-type enzyme were preserved (Figures 2b and 4d). In contrast, the E617N variant, which also lacks a negative charge but has a shorter side chain, showed only 7% of the wild-type catalytic efficiency (Table 1).

Why, then, does LGOX fail to recognize amino acids other than L-glutamate? Aspartate and asparagine are too short to interact with R305. Basic amino acids and glutamine cannot bind due to the presence of R305 and H312, which would result in steric or electrostatic repulsion. Additionally, the substrate-binding pocket of LGOX is hydrophilic, making it unfavorable for the binding of hydrophobic amino acids. While LAAOs that bind hydrophobic amino acids or LysOX possess the hydrophobic hole surrounding the β and γ positions of the substrate side chain (Kondo et al., 2020), LGOX lacks such a feature (Figure S3). The hydrophobic hole of LAAOs with broad substrate specificity, such as LAAO from *Calloselasma rhodostoma* (CrLAAO) (Pawelek et al., 2000), interacts with the hydrophobic region of the substrate side chain and contributes to recognizing various hydrophobic amino acids (Figure S3a) (Kondo et al., 2020; Pawelek et al., 2000). L-phenylalanine oxidase from *Pseudomonas* sp. P-501 (PAO), which shows high activity for L-phenylalanine and L-tyrosine, and relatively low activity for L-methionine and L-tryptophan (Ida et al., 2011; Koyama, 1982), seems to have a partially broken hydrophobic hole (Figure S3b). T313 exists at a corner of its hydrophobic hole and is slightly away from the substrate. However, the oxygen atom of T313 faces a different direction from the hydrophobic hole, and thus, the hydrophobic nature of the hole is maintained. Therefore, the hydrophobic hole of PAO is wider than that of other LAAOs and can accommodate large hydrophobic amino acids, such as L-phenylalanine and L-tryptophan, but is unfavorable for binding small hydrophobic amino acids. The LysOX recognizes the hydrophobic side chain arm of L-lysine through a narrow hydrophobic hole (Figure S3c) (Kondo et al., 2020). In contrast to these LAAOs, LGOX does not have the hydrophobic hole (Figure S3d). E617 exists at the corresponding position of F439 of LysOX and prevents amino acids with a hydrophobic group at β and/or γ positions from being stably positioned for catalysis. These structural characteristics together explain the high substrate specificity of LGOX for L-glutamate.

While the substrate access path to the active site in LysOX is funnel-shaped (Kondo et al., 2020), LGOX features a generally wider access pathway. In LysOX, upon substrate binding, the indole ring of W371, which is located at the innermost point of the funnel, shifts to block the entrance to the substrate-binding site (Kondo et al., 2020). In contrast, the corresponding residue in LGOX, W564, does not undergo such a conformational change. A recent structural study of AncLLysO, which is an artificial LysOX designed using the ASR method, reported that substrate binding induces a conformational change of a plug loop formed by four residues near the substrate binding site (Sugiura et al., 2021). However, no such loop is present in LGOX. Instead, LGOX utilizes a large conformational shift of the entrance loop to regulate access to the substrate-binding site. In the substrate-bound structures of wild-type LGOX, E617Q, and R305E, the entrance loop adopts a similar conformation that effectively seals off the tunnel leading to the substrate-binding site (Figures 1b–d and 4a). By contrast, in the substrate-free state, the entrance loop displays multiple conformations. The entrance loops of substrate-free wild-type LGOX and the E617Q variant share similar conformations, leaving the tunnel to the active site open (Figures 1b–d and 4a). In the E617F and E617K variants, the entrance loop exhibits alternative conformations, both open and closed states of the tunnel (Figure 6a,b). The conformation of the entrance loop in the R305E protein differs from all others and blocks the tunnel. Importantly, in all these crystal structures, the entrance loop does not make contact with neighboring molecules, and differences in crystal packing cannot explain the conformational variability. Notably, the space groups differ between the substrate-bound wild-type LGOX and the E617Q variant structures, as well as between the substrate-free E617F and E617K variant structures. However, wild-type LGOX shares the same space group in both substrate-bound and substrate-free forms. These observations indicate that the conformational differences in the entrance loop are not artifacts of crystal packing. Given the wide substrate access pathway in LGOX, regulation of tunnel opening and closing cannot be achieved by a single amino acid side-chain movement, as in LysOX (Kondo et al., 2020). Instead, a large-scale conformational change of the entrance loop is required. It is likely that in the substrate-free state, the entrance loop remains flexible, allowing the tunnel to alternate between open and closed conformations. A similar open-close motion of the loop at the entrance of the tunnel has recently been reported in the ligand-free structures of L-arginine oxidase from *Pseudomonas* sp. TPU 7192 determined by X-ray and CryoEM (Yamaguchi et al., 2025), supporting this idea. Upon substrate binding, the entrance loop adopts a closed conformation, sealing off the tunnel to stabilize substrate engagement.

1469896x, 2026, 1, Downloaded from https://onlinelibrary.wiley.com/doi/10.1002/pro.70432 by The University Of Osaka, Wiley Online Library on [07/01/2026]. See the Terms and Conditions (https://onlinelibrary.wiley.com/terms-and-conditions) on Wiley Online Library for rules of use; OA articles are governed by the applicable Creative Commons License

The E617F and E617K variants exhibit high activity toward L-tyrosine, but low activity toward other L-amino acids (Table 1). Although they retain slight activity toward L-phenylalanine and L-glutamate, it is less than 16% of that for L-tyrosine, indicating conversion into tyrosine-specific oxidases. LGOX has also been successfully converted into an arginine-specific oxidase through the R305E mutation (Yano et al., 2021). In contrast, no LysOX mutant proteins with altered substrate specificity and high selectivity have been obtained. The D212A/D315A LysOX mutant gained activity toward L-phenylalanine but also retained over 50% activity toward L-arginine, L-tyrosine, and L-tryptophan, indicating low substrate specificity (Kondo et al., 2020). LGOX lacks a hydrophobic hole, making it unsuitable for binding hydrophobic or small side-chain amino acids (Figure S3). However, its rather wide substrate-binding pocket allows greater mutational flexibility, enabling the potential development of highly specific or novel amino acid oxidases through combinations of mutations. Thus, LGOX serves as a suitable template for engineering enzymes with tailored substrate specificity.

4 | METHODS

4.1 | Strains and plasmids

The bacterial strains and the plasmids used in this study are listed in Table S2.

4.2 | Site-directed mutagenesis

The expression vector of LGOX (pGOx_mal1) was constructed as described previously (Utsumi et al., 2012). Genes of H312A, H312E, D433A, D433E, D433K, and 19 E617X variants were produced by site-directed mutagenesis by inverse PCR using KOD Plus Neo (Takara, Japan), pGOx_mal1 as a template, and oligonucleotide primers listed in Table S3. The template plasmid was digested with Dpn I at 37°C for 1 h. The plasmid carrying LGOX variants was transformed into *E. coli* JM109. The introduction of the mutation was confirmed by DNA sequencing.

4.3 | Purification of LGOX

Escherichia coli JM109 cells harboring pGOx_mal1, pGOx_mal1_H312X, D433X, or E617X were precultured at 37°C for 16 h in 5 mL of LB medium containing 50 μg mL^{-1} ampicillin. The preculture at a final concentration of 0.1% was transferred to 1 L of 2 × YT medium containing 50 μg mL^{-1} ampicillin and incubated at 22°C for 24 h. Expression of LGOX was induced by the addition of 0.1 mM IPTG for 22 h at 22°C. Cells were harvested by centrifugation and stored at −80°C until use. The pellet was thawed and resuspended in 20 mM potassium phosphate buffer (KPB) at pH 7.4 and sonicated at 150 W for 15 min at 4°C. After removal of cell debris by centrifugation, the supernatant of LGOX was brought to 30% saturation with ammonium sulfate for 30 min on ice. After removal of the precipitate, the supernatant was brought to 60% saturation with ammonium sulfate for 30 min on ice. The precipitate was collected by centrifugation, dissolved in 20 mM KPB (pH 7.4), and dialyzed for 16 h against buffer A (20 mM Tris–HCl (pH 7.4) with 200 mM NaCl and 1 mM EDTA). The solution was loaded on an amylose resin (New England Biolabs, Ipswich, MA, USA) equilibrated with buffer A, and the enzyme was eluted with buffer A containing 10 mM maltose. The fractions containing LGOX were concentrated, mixed with metalloprotease from *S. griseus* (Kaken Pharmaceutical Co., Ltd., Tokyo, Japan) at 4% (w/w) relative to the protein, and stored at 30°C for 18 h for maturation. Then, the mixture was incubated at 60°C for 20 min to denature the protease and centrifuged to remove the precipitate.

The protein samples for crystallization were further purified by anion exchange chromatography followed by size exclusion chromatography. The supernatant was loaded on a DEAE Toyopearl 650 M column (Tosoh Corp., Tokyo, Japan) equilibrated with 20 mM KPB (pH 7.4) containing 100 mM NaCl and eluted with 20 mM KPB (pH 7.4) containing 200 mM NaCl. The fractions containing LGOX were concentrated, applied to a Sephacryl S 300 HR column (Cytiva) equilibrated with 20 mM KPB (pH 7.4), and eluted. The peak fractions corresponding to the LGOX dimer were applied to a High Load 26/60 Superdex 200 pg. column (Cytiva) or Superdex 200 Increase 10/300 GL column (Cytiva) equilibrated with 20 mM Tris–HCl pH 7.5 containing 300 mM NaCl and eluted.

The protein concentration was determined by the Bradford method using a Bio-Rad Protein Assay kit (Bio-Rad Laboratories, Inc., Hercules, CA, USA) with bovine serum albumin as a standard. The purity of the enzyme was assessed by SDS-PAGE (15%) and Native-PAGE (7.5%).

4.4 | Enzyme assay

The enzyme activity was measured by detecting hydrogen peroxide using the 4-aminoantipyrine phenol method or by monitoring α-keto acid using the 3-methyl-2-benzothiazolinone hydrazone (MBTH) method as described previously (Yano et al., 2021). The protein concentrations were determined by the Bradford method using a Bio-Rad Protein Assay kit (Bio-Rad Laboratories, Inc., Hercules, CA, USA) with bovine serum albumin as a standard.

1469896x, 2026, 1, Downloaded from https://onlinelibrary.wiley.com/doi/10.1002/pro.70432 by The University Of Osaka, Wiley Online Library on [07/01/2026]. See the Terms and Conditions (https://onlinelibrary.wiley.com/terms-and-conditions) on Wiley Online Library for rules of use; OA articles are governed by the applicable Creative Commons License

4.5 | Determination of substrate specificity

The substrate specificity was determined by measuring enzyme activities for 20 L-α-amino acids at pH 7.4 or 8.0 using the 4-aminoantipyrine phenol method (Yano et al., 2021).

4.6 | Determination of optimum pH and temperature

Optimum pH was determined by measuring enzyme activity (LGOX E617K and E617F for 5 mM L-tyrosine at 40°C; wild-type LGOX for 1 mM L-glutamate at 50°C) using the MBTH method; 70 mM KPB (pH 6–8) and 70 mM borate-NaOH buffer (pH 8–10) were used for LGOX E617K, and a universal buffer pH 6–10 (50 mM boric acid, 50 mM citric acid, 50 mM acetic acid, 50 mM NaH_2PO_4, 50 mM CAPS, and 25 mM HEPES) adjusted by 5 mol L^{-1} NaOH solution was used for wild-type LGOX and LGOX E617F. The optimum temperature was determined by measuring enzyme activity (LGOX E617K and E617F for 5 mM L-tyrosine; wild-type LGOX for 1 mM L-glutamate) at 20–70°C in 70 mM KPB (pH 7.4) using the MBTH method.

4.7 | Measurement of residual activity

The thermostability was evaluated by measuring enzyme activity (LGOX E617K, E617F for L-tyrosine; wild-type LGOX for L-glutamate) by the MBTH method at optimum assay conditions after a 1 h preincubation at various temperatures (30°C–90°C). The residual activity was defined as the relative activity compared to the enzyme activity after preincubation at 0°C for 1 h, which was set as 100%.

4.8 | Determination of the kinetic parameters

The enzyme activity at various concentrations of substrate was measured by the 4-aminoantipyrine phenol method at the optimum assay condition of each enzyme. Kinetic parameters were determined by fitting the data to the Michaelis–Menten equation using Solver in Microsoft Excel (Microsoft Co.). FAD content was estimated by the ratio of OD_{280} and OD_{450} for wild-type, E617Q, E617F, and E617K. The ratio values of the mutants were within 90% of the wild type. Therefore, the FAD content of these mutant proteins did not significantly affect their kinetic parameters determined in this study.

4.9 | Preparation of crystals

Crystallization screening was performed at 277 K and 293 K by the sitting-drop vapor diffusion method using the following screening kits: Wizard Classic 1 and 2, Wizard Classic 3 and 4 (Rigaku), Crystal Screen 1 and 2, and PEG RX 1 and 2 (Hampton Research). Each drop was prepared by mixing 0.5 μL protein solution (10 mg mL^{-1}) with an equal volume of reservoir solution and was equilibrated against 85 μL of reservoir solution using Compact 300 Crystallization Plates (XJR). The crystallization conditions were optimized by screening additives and the concentration of the precipitants and additives, if needed. The crystals used for preparation of the L-glutamate complex of LGOX were obtained at 293 K from drops prepared by mixing protein solution (10 mg mL^{-1}) containing 20 mM KPB (pH 7.4) with an equivalent volume of reservoir solution containing 0.1 M CAPS (pH 10.5), 1.2 M NaH_2PO_4, 0.8 M K_2HPO_4, and 0.2 M Li_2SO_4. The best crystals of LGOX E617Q were grown at 293 K from drops prepared by mixing protein solution (8.5 mg mL^{-1}) containing 20 mM KPB (pH 7.4) with an equivalent volume of reservoir solution containing 0.1 M Tris–HCl (pH 7.0), 2.5 M NaCl, and 0.2 M $MgCl_2$ for the analysis of substrate-free structure and 0.1 M Tris–HCl (pH 7.0), 12% (w/v) PEG8000, and 0.2 M $MgCl_2$ for the analysis of L-glutamate complex. The crystals of LGOX E617F suitable for X-ray analysis were grown at 293 K from drops prepared by mixing protein solution (10 mg·mL^{-1}) containing 20 mM KPB (pH 7.4) with an equivalent volume of reservoir solution containing 20% (w/v) PEG3350, and 0.02 M $ZnCl_2$. The crystals of LGOX E617K suitable for X-ray analysis were obtained at 277 K from drops prepared by mixing protein solution (9.6 mg mL^{-1}) containing 20 mM KPB (pH 7.4) with an equivalent volume of reservoir solution containing 0.1 M CAPS (pH 10.5), 20% (w/v) PEG8000, and 0.02 M NaCl. The substrate complex crystals were prepared by the soaking method. The crystals were soaked in a reservoir solution containing 10% (v/v) glycerol and 5–10 mM L-glutamate and were stored at 293 K until the yellow color disappeared (typically 5 min).

4.10 | Data collection and structure determination

The X-ray data were corrected at SPring-8 beamlines, BL41XU (Harima, Japan) with the approval of the Japan Synchrotron Radiation Research Institute (Proposal Nos 2021A2736, 2021B2738, 2022A2740, 2023A2720, and 2023A2721). The crystals were transferred into liquid nitrogen for freezing. The E617F, E617K, and E617Q variant crystals were soaked in a cryo-protectant solution containing 10% (v/v) glycerol

1469896x, 2026, 1, Downloaded from https://onlinelibrary.wiley.com/doi/10.1002/pro.70432 by The University Of Osaka, Wiley Online Library on [07/01/2026]. See the Terms and Conditions (https://onlinelibrary.wiley.com/terms-and-conditions) on Wiley Online Library for rules of use; OA articles are governed by the applicable Creative Commons License

and 90% (v/v) of the reservoir solution for several seconds before freezing. The diffraction data were collected under nitrogen gas flow at 100 K. The diffraction data were indexed and integrated with MOSFLM (Battye et al., 2011) and were scaled with AIMLESS (Evans, 2006). The diffraction data statistics are summarized in Table S1. The initial phase was obtained by the molecular replacement method with Phaser (McCoy et al., 2007) using the structure of wild-type LGOX (PDB: 2E1M) as a search model. The atomic models were built with Coot (Emsley et al., 2010) and refined with PHENIX (Adams et al., 2010). The structural refinement statistics are shown in Table S1.

AUTHOR CONTRIBUTIONS

Yuka Ueda: Investigation; visualization; writing – original draft. **Yoshika Yano:** Investigation; visualization; writing – original draft. **Natsume Nakayama:** Investigation. **Norihiro Takekawa:** Investigation. **Kenji Inagaki:** Conceptualization; project administration; resources; supervision; writing – original draft; writing – review and editing. **Katsumi Imada:** Conceptualization; investigation; project administration; supervision; visualization; writing – original draft; writing – review and editing.

ACKNOWLEDGMENTS

The authors thank the SPring-8 beamline staff for technical help in the use of beamline BL41XU. This work was supported by JSPS KAKENHI Grant Numbers 21K05278 (to Kenji Inagaki).

CONFLICT OF INTEREST STATEMENT

The authors declare no conflict of interest.

DATA AVAILABILITY STATEMENT

The atomic coordinates and structure factors have been deposited in Protein Data Bank (https://www.pdb.org) with the access codes of 9W54, 9W55, 9W56, 9W57, and 9W58. Other data that support the findings of this study are available from the corresponding author upon reasonable request.

ORCID

Katsumi Imada https://orcid.org/0000-0003-1342-8885

REFERENCES

Adams PD, Afonine PV, Bunkóczi G, Chen VB, Davis IW, Echols N, et al. PHENIX: a comprehensive python-based system for macromolecular structure solution. Acta Crystallogr D Biol Crystallogr. 2010;58:1948–54.

Al-Shameri A, Schmermund L, Sieber V. Current advances in the enzyme engineering of O_2-dependent enzymes–boosting the versatility and applicability of oxygenases and oxidases. ChemCatChem. 2024;16:e202301109.

Amano M, Mizuguchi H, Sano T, Kondo H, Shinyashiki K, Inagaki J, et al. Recombinant expression, molecular characterization and crystal structure of antitumor enzyme, l-lysine α-oxidase from *Trichoderma viride*. J Biochem. 2015;157:549–59.

Arima J, Sasaki C, Sakaguchi C, Mizuno H, Tamura T, Kashima A, et al. Structural characterization of l-glutamate oxidase from *Streptomyces* sp. X-119-6. FEBS J. 2009;276:3894–903.

Arima J, Tamura T, Kusakabe H, Ashiuchi M, Yagi T, Tanaka H, et al. Recombinant expression, biochemical characterization and stabilization through proteolysis of an L-glutamate oxidase from *Streptomyces* sp. X-119-6. J Biochem. 2003;134:805–12.

Battye TGG, Kontogiannis L, Johnson O, Powell HR, Leslie AGW. iMOSFLM: a new graphical interface for diffraction image processing with MOSFLM. Acta Crystallogr D Biol Crystallogr. 2011;67:271–81.

Böhmer A, Müllar A, Passarge M, Liebs P, Honeck H, Müllar HG. A novel l-glutamate oxidase from *Streptomyces endus*. Purification and properties. Eur J Biochem. 1989;182:327–32.

Chen HS, Wang YM, Huang WT, Huang KF, Tsai IH. Cloning, characterization and mutagenesis of Russell's viper venom L-amino acid oxidase: insights into its catalytic mechanism. Biochimie. 2012;94:335–44.

Duerre JA, Chakrabarty S. L-amino acid oxidases of *Proteus rettgeri*. J Bacteriol. 1975;121:656–63.

El-Sayed AS, Shindia AA, Zaher YA. Purification and characterization of L-amino acid oxidase from the solid-state grown cultures of *Aspergillus oryzae* ASH. Microbiology. 2013;82:762–71.

Emsley P, Lohkamp B, Scott WG, Cowtan K. Features and development of coot. Acta Crystallogr D Biol Crystallogr. 2010;66:486–501.

Evans P. Scaling and assessment of data quality. Acta Crystallogr D Biol Crystallogr. 2006;62:72–82.

Füller JJ, Röpke R, Krausze J, Rennhack KE, Daniel NP, Blankenfeldt W, et al. Biosynthesis of violacein, structure and function of L-tryptophan oxidase VioA from *Chromobacterium violaceum*. J Biol Chem. 2016;291:20068–84.

Geueke B, Hummel W. A new bacterial l-amino acid oxidase with a broad substrate specificity: purification and characterization. Enzym Microb Technol. 2002;31:77–87.

Ida K, Suguro M, Suzuki H. High resolution X-ray crystal structures of L-phenylalanine oxidase (deaminating and decarboxylating) from *Pseudomonas* sp. P-501. Structures of the enzyme-ligand complex and catalytic mechanism. J Biochem. 2011;150:659–69.

Izidoro LFM, Sobrinho JC, Mendes MM, Costa TR, Grabner AN, Rodrigues VM, et al. Snake venom l-amino acid oxidases: trends in pharmacology and biochemistry. Biomed Res Int. 2014;2014:196754.

Kamei T, Asano K, Suzuki H, Matsuzaki M, Nakamura S. L-glutamate oxidase from *Streptomyces violacens*. I. Production, isolation, and some properties. Chem Pharm Bull. 1983;31:1307–14.

Kasai K, Ishikawa T, Nakamura T, Miura T. Antibacterial properties of L-amino acid oxidase: mechanisms of action and perspectives for therapeutic applications. Appl Microbiol Biotechnol. 2015;99:7847–57.

Kasai K, Nakano M, Ohishi M, Nakamura T, Miura T. Antimicrobial properties of L-amino acid oxidase: biochemical features and biomedical applications. Appl Microbiol Biotechnol. 2021;105:4819–32.

Kondo H, Kitagawa M, Matsumoto Y, Saito M, Amano M, Sugiyama S, et al. Structural basis of strict substrate recognition of L-lysine α-oxidase from *Trichoderma viride*. Protein Sci. 2020;29:2213–25.

Koyama H. Purification and characterization of a novel L-phenylalanine oxidase (deaminating and decarboxylating) from *Pseudomonas* sp. P-501. J Biochem. 1982;92:1235–40.

Kusakabe H, Kodama K, Kuninaka A, Yoshino H, Misono H, Soda K. A new antitumor enzyme, l-lysine oxidase from *Trichoderma viride*. Purification and enzymological properties. J Biol Chem. 1980;255:976–81.

Kusakabe H, Midorikawa Y, Fujishima T, Kuninaka A, Yoshino H. Purification and properties of a new enzyme, l-glutamate

1469896x, 2026, 1, Downloaded from https://onlinelibrary.wiley.com/doi/10.1002/pro.70432 by The University Of Osaka, Wiley Online Library on [07/01/2026]. See the Terms and Conditions (https://onlinelibrary.wiley.com/terms-and-conditions) on Wiley Online Library for rules of use; OA articles are governed by the applicable Creative Commons License

oxidase, from *Streptomyces sp*. X-119-6 grown on wheat bran. Agric Biol Chem. 1983;47:1323–8.
Liu Q, Ma X, Cheng H, Xu N, Liu J, Ma Y. Co-expression of L-glutamate oxidase and catalase in *Escherichia coli* to produce α-ketoglutaric acid by whole-cell biocatalyst. Biotechnol Lett. 2017;39:913–9.
Lukasheva EV, Babayeva G, Karshieva SS, Zhdanov DD, Pokrovsky VS. L-lysine α-oxidase: enzyme with anticancer properties. Pharmaceuticals (Basel). 2021;14:1070.
Mandal S, Bhattacharyya D. Two l-amino acid oxidase isoenzymes from Russell's viper (*Daboia russelli russelli*) venom with different mechanisms of inhibition by substrate analogs. FEBS J. 2008;275:2078–95.
Matsui D. Development of oxidoreductases for amino acid quantification and mutagenesis techniques for heterologous soluble expression: screening and selection strategies. Biosci Biotechnol Biochem. 2023;87:473–81.
Matsui D, Terai A, Asano Y. L-arginine oxidase from *Pseudomonas sp*. TPU 7192: characterization, gene cloning, heterologous expression, and application to L-arginine determination. Enzym Microb Technol. 2016;82:151–7.
McCoy AJ, Grosse-Kunstleve RW, Adams PD, Winn MD, Storoni LC, Read RJ. Phaser crystallographic software. J Appl Crystallogr. 2007;40:658–74.
Mizon J, Biserte G, Boulanger P. Quelques propriétés de la l-amino acide oxydase du foie de dindon (Meleagris gallopavo l.). Biochim Biophys Acta. 1970;212:33–42.
Moustafa IM, Foster S, Lyubimov AY, Vrielink A. Crystal structure of LAAO from *Calloselasma rhodostoma* with an L-phenylalanine substrate: insights into structure and mechanism. J Mol Biol. 2006;364:991–1002.
Nakano S, Minamino Y, Hasebe F, Ito S. Deracemization and stereoinversion to aromatic d-amino acid derivatives with ancestral l-amino acid oxidase. ACS Catal. 2019;9:10152–8.
Nakano S, Niwa M, Asano Y, Ito S. Following the evolutionary track of a highly specific l-arginine oxidase by reconstruction and biochemical analysis of ancestral and native enzymes. Appl Environ Microbiol. 2019;85:e00459-19.
Nasu S, Wicks FD, Gholson RK. L-aspartate oxidase, a newly discovered enzyme of *Escherichia coli*, is the B protein of quinolinate synthetase. J Biol Chem. 1982;257:626–32.
Pawelek PD, Cheah J, Coulombe R, Macheroux P, Ghisla S, Vrielink A. The structure of l-amino acid oxidase reveals the substrate trajectory into an enantiomerically conserved active site. EMBO J. 2000;19:4204–15.
Pollegioni L, Motta P, Molla G. L-amino acid oxidase as biocatalyst: a dream too far? Appl Microbiol Biotechnol. 2013;97:9323–41.
Sugiura S, Nakano S, Niwa M, Hasebe F, Matsui D, Ito S. Catalytic mechanism of ancestral L-lysine oxidase assigned by sequence data mining. J Biol Chem. 2021;297:101043.
Ullah A. Structure-function studies and mechanism of action of snake venom l-amino acid oxidases. Front Pharmacol. 2020;11:110.
Utsumi T, Arima J, Sakaguchi C, Tamura T, Sasaki C, Kusakabe H, et al. Arg305 of *Streptomyces* L-glutamate oxidase plays a crucial role for substrate recognition. Biochem Biophys Res Commun. 2012;417:951–5.
Wang L, Peng R, Tian Y, Liu M, Yao Q. Isolation and characterization of a novel L-glutamate oxidase with strict substrate specificity from *Streptomyces diastatochromogenes*. Biotechnol Lett. 2017;39:523–8.
Wei JF, Yang HW, Wei XL, Qiao LY, Wang WY, He SH. Purification, characterization, and biological activities of the L-amino acid oxidase from *Bungarus fasciatus* snake venom. Toxicon. 2009;54:262–71.
Wei XL, Wei JF, Li T, Qiao LY, Liu YL, Huang T, et al. Purification, characterization and potent lung lesion activity of an L-amino acid oxidase from *Agkistrodon blomhoffii ussurensis* snake venom. Toxicon. 2007;50:1126–39.
Yamaguchi H, Takahashi K, Numoto N, Suzuki H, Tatsumi M, Kamegawa A, et al. Open and closed structures of L-arginine oxidase by cryo-electron microscopy and X-ray crystallography. J Biochem. 2025;177:27–36.
Yano Y, Matsuo S, Ito N, Tamura T, Kusakabe H, Inagaki K, et al. A new L-arginine oxidase engineered from L-glutamate oxidase. Protein Sci. 2021;30:1044–55.
Yu Z, Qiao H. Advances in non-snake venom L-amino acid oxidase. Appl Biochem Biotechnol. 2012;167:1–13.
Zhang YJ, Wang JH, Lee WH, Wang Q, Liu H, Zheng YT, et al. Molecular characterization of *Trimeresurus stejnegeri* venom L-amino acid oxidase with potential anti-HIV activity. Biochem Biophys Res Commun. 2003;309:598–604.

SUPPORTING INFORMATION

Additional supporting information can be found online in the Supporting Information section at the end of this article.

How to cite this article: Ueda Y, Yano Y, Nakayama N, Takekawa N, Inagaki K, Imada K. Substrate recognition mechanisms of L-glutamate oxidase from *Streptomyces* sp. and its conversion to L-tyrosine oxidase. Protein Science. 2026;35(1):e70432. https://doi.org/10.1002/pro.70432

1469896x, 2026, 1, Downloaded from https://onlinelibrary.wiley.com/doi/10.1002/pro.70432 by The University Of Osaka, Wiley Online Library on [07/01/2026]. See the Terms and Conditions (https://onlinelibrary.wiley.com/terms-and-conditions) on Wiley Online Library for rules of use; OA articles are governed by the applicable Creative Commons License